

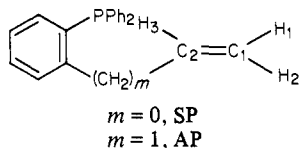
Closo and Hyper-Closo Ten-Vertex Ruthenacarboranes Containing Chelating Alkenylphosphine Ligands

C. W. Jung, R. T. Baker, C. B. Knobler, and M. F. Hawthorne*

Contribution from the Department of Chemistry, University of California, Los Angeles, California 90024. Received January 29, 1980

Abstract: Reactions of [*hyper-closo*-2-R¹-3-R²-6,6-(PPh₃)₂-6,2,3-RuC₂B₇H₇] (I) with (*o*-styryl)diphenylphosphine (R^{1,2} = H, CH₃; R¹ = H, R² = Ph), (*o*-allylphenyl)diphenylphosphine (R^{1,2} = H, CH₃), and Ph_{3-n}P(CH₂CH₂CH=CH₂)_n (n = 1, 2; R^{1,2} = CH₃) afforded the 16e⁻ ruthenacarborane complexes [*hyper-closo*-RuL(C₂B₇H₇R¹R²)] (IIa-g), in which the alkenylphosphine (L) functions as a bidentate ligand. The crystal structure of [2,3-(CH₃)₂-6-(CH₂=CHCH₂C₆H₄Ph₂P)-6,2,3-RuC₂B₇H₇] (IIId) was determined from three-dimensional X-ray counter data. The complex crystallizes in the monoclinic system, space group *P*2₁/*c*, with *a* = 11.740 (3) Å, *b* = 15.185 (5) Å, *c* = 21.748 (7) Å, β = 137.43 (2)°, and *Z* = 4. Refinement of 4168 independent reflections with *I* > 3σ(*I*) led to a final value of *R* = 4.0%. The structure of this complex may best be described in terms of a C₂B₇ fragment of arachno geometry which occupies nine vertices of an 11-vertex octadecahedron with a ruthenium atom in a "nonvertex" position and within bonding distance of six atoms in the open face. The observed distortion from the common ten-vertex bicapped square antiprismatic structure is thought to be a result of the perturbation of the polyhedral skeletal bonding induced by the 16-electron Ru^{II} center. Reaction of IIb with carbon monoxide displaced the coordinated alkenyl side chain to yield the 18e⁻ Ru^{II} complex [*closo*-6,6-(CO)₂-6-L-6,2,3-RuC₂B₇H₉] (IIIa) [L = (*o*-allylphenyl)diphenylphosphine]. Reactions of Ph_{3-n}P(CH₂CH₂CH=CH₂)_n (n = 1, 2) with [*hyper-closo*-6,6-(PPh₃)₂-6,2,3-RuC₂B₇H₉] produced the fluxional complexes [*closo*-6,6-L₂-6,2,3-RuC₂B₇H₉] (IVa,b) which exhibit butenyl side-chain exchange and undergo *closo*-*hyper-closo* equilibria as evidenced by variable temperature multinuclear FT NMR spectroscopy. The reactions of IVa,b with carbon monoxide are also discussed.

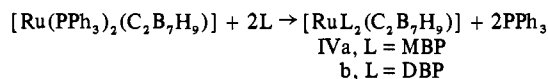
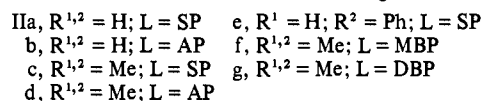
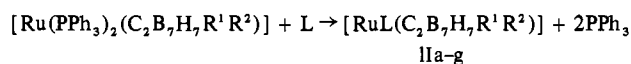
As part of our study of metallocarborane-catalyzed homogeneous hydrogenation and isomerization of alkenes,^{1,2} we have attempted to isolate or detect possible intermediates in the catalytic cycle.³ Although we have previously noted that the unsaturated ruthenacarboranes [Ru(PPh₃)₂(C₂B_nH_{n+2})] (n = 7,⁴ 9²) react with electron-deficient alkenes, we were unable to isolate alkene-metallocarborane complexes because of their instability. To overcome this difficulty, the potentially chelating alkenylphosphines⁵ (*o*-styryl)diphenylphosphine (SP),⁶ (*o*-allylphenyl)diphenylphosphine (AP),⁷ and Ph_{3-n}P(CH₂CH₂CH=CH₂)_n [n = 1, but-3-enyl-di-



phenylphosphine (MBP); n = 2, di(but-3-enyl)phenylphosphine (DBP)⁸ were used to prepare derivatives of the above ruthenacarboranes. This paper describes the synthesis and properties of such alkenylphosphine complexes prepared from [2R-R¹-3-R²-6,6-(PPh₃)₂-6,2,3-RuC₂B₇H₇] (Ia-c, R^{1,2} = H or Me; R¹ = H, R² = Ph).

The complex [2,3-(CH₃)₂-6-(CH₂=CHCH₂C₆H₄Ph₂P)-6,2,3-RuC₂B₇H₇] was the subject of a single-crystal X-ray dif-

Scheme I. Synthesis of Closo and Hyper-Closo Ten-Vertex Ruthenacarborane Complexes



fraction study, which revealed several interesting structural features. Unlike previously isolated metal complexes derived from the 1,3-dicarba-*arachno*-nonaborane(13) cage system,⁹ this complex has the metal within bonding distance of *all six atoms* in the open face. Distortion from the standard *closo* structure was anticipated as this *n*-vertex polyhedron contains only 2*n* skeletal bonding electrons, as does [*hyper-closo*-(η⁵-C₅H₅)Fe]₂C₂B₆H₈.¹⁰

The complexes [*closo*-6,6-L₂-6,2,3-RuC₂B₇H₉] (L = MBP or DBP) were the subject of a variable temperature multinuclear FT NMR study which demonstrated the existence of two types of exchange processes. The first involves exchange of metal-coordinated and uncoordinated butenyl side chains, while the second involves phosphine ligand dissociation with concomitant polyhedral rearrangement (*closo*-*hyper-closo* equilibrium).

Results and Discussion

Synthesis, Reactivity, and Spectral Data for Hyper-Closo Ruthenacarboranes. The reactions of [Ru(PPh₃)₂(C₂B₇H₇R¹R²)] with SP or AP (R^{1,2} = H or Me; R¹ = H, R² = Ph, SP only) and MBP or DBP (R^{1,2} = Me) afforded the deep-red, crystalline compounds [RuL(C₂B₇H₇R¹R²)] (IIa-g, L = alkenyl tertiary phosphine; see Scheme I). Elemental analyses and mass-spectral data agreed with the proposed empirical formulas for IIa-g. Except for L = DBP (IIg), the infrared spectra of IIa-g contained no bands near 1630 cm⁻¹ due to ν_{C=C} for a free alkene group.

(9) T. A. George and M. F. Hawthorne, *J. Am. Chem. Soc.*, **91**, 5475 (1969); D. St. Clair, A. Zalkin, and D. H. Templeton, *Inorg. Chem.*, **11**, 377 (1972).

(10) K. P. Callahan, W. J. Evans, F. Y. Lo, C. E. Strouse, and M. F. Hawthorne, *J. Am. Chem. Soc.*, **97**, 296 (1975).

(1) T. E. Paxson and M. F. Hawthorne *J. Am. Chem. Soc.*, **96**, 4674 (1974); R. E. King, D. C. Busby, M. S. Delaney, T. B. Marder, B. S. Anfield, R. T. Baker, J. A. Long, C. B. Kreimendahl, W. C. Kalb, T. E. Paxson, and M. F. Hawthorne, *ibid.*, to be submitted.

(2) E. H. S. Wong and M. F. Hawthorne, *J. Chem. Soc., Chem. Commun.*, 257 (1976); *Inorg. Chem.*, **17**, 2863 (1978).

(3) C. W. Jung and M. F. Hawthorne, *J. Am. Chem. Soc.*, **102**, 3024 (1980).

(4) C. W. Jung and M. F. Hawthorne, *J. Chem. Soc., Chem. Commun.*, 499 (1976); C. W. Jung, R. T. Baker, and M. F. Hawthorne, *J. Am. Chem. Soc.*, in press.

(5) For a review of metal complexes of these ligands see D. I. Hall, J. H. Ling, and R. S. Nyholm, *Struct. Bonding (Berlin)*, **15**, 3 (1973).

(6) L. V. Interrante, M. A. Bennett, and R. S. Nyholm, *Inorg. Chem.*, **5**, 2212 (1966).

(7) M. A. Bennett, J. Chatt, G. J. Erskine, J. Lewis, R. F. Long, and R. S. Nyholm, *J. Chem. Soc. A*, 501 (1967).

(8) P. W. Clark, J. L. S. Curtis, P. E. Garrou, and G. E. Hartwell, *Can. J. Chem.*, **52**, 1714 (1974).

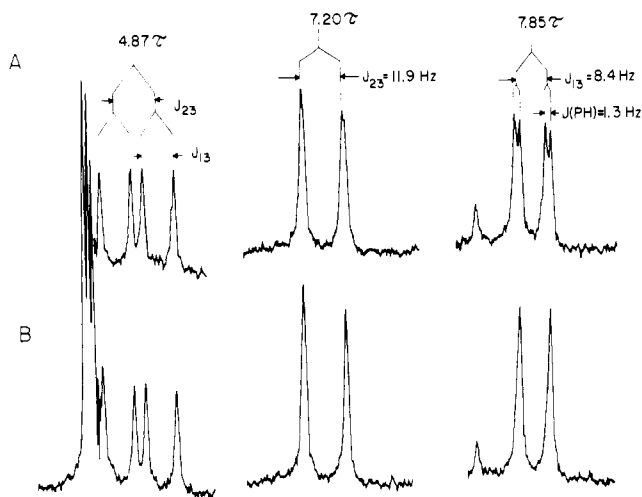


Figure 1. (A) The 100-MHz ^1H NMR spectrum of $[\text{Ru}(\text{SP})(\text{C}_2\text{B}_7\text{H}_9)]$ (IIa) in CD_2Cl_2 . (B) Same with ^{31}P decoupling (triplet at τ 4.72 is due to residual CHDCl_2).

Instead, medium to weak bands at 1470 and 1260 cm^{-1} assignable to a coordinated alkene were observed.^{11,12}

The NMR spectra of complexes IIa–g were also consistent with coordination of the alkene side chain to the ruthenium atom. The alkenyl proton resonances were shifted 1.4–3.7 ppm upfield from the corresponding resonances of the free ligand. With ^{31}P decoupling, the alkenyl proton resonances of $[\text{Ru}(\text{SP})(\text{C}_2\text{B}_7\text{H}_9)]$ (IIa) appeared as a first-order AMX spin system with no detectable geminal coupling between H_1 and H_2 (Figure 1). These alkenyl signals were assigned by assuming that the magnitudes of trans vicinal couplings (J_{2-3}) remain larger than the corresponding cis couplings (J_{1-3}) upon complexation of the alkenyl group to ruthenium. The alkenyl coupling constants of IIa–g were smaller than those in the free ligands^{8,13,14} and similar to those found in other transition-metal complexes containing chelating alkenylphosphines or -arsines.^{15,16} In the $^{13}\text{C}\{^1\text{H}\}$ NMR spectra, the alkenyl carbons of IIa–g appeared approximately 42–60 ppm upfield from those of the free phosphine.¹⁷ Off-resonance decoupled and proton-coupled spectra (for sufficiently soluble compounds) were used to assign these resonances.

The ^{11}B NMR spectra of compounds IIa–g were consistent with the presence of an asymmetric carboranyl ligand (see Figure 2). Those of IIc,g contained seven doublets ($J_{\text{B-H}} \approx 120\text{ Hz}$) of roughly equal areas and the spectra of IIa–e were similar, but not as well resolved. As in the parent, $[\text{Ru}(\text{PPh}_3)_2(\text{C}_2\text{B}_7\text{H}_7\text{R}^2)]$,⁴ the complexes IIa–g exhibited resonances at about 107 ppm (relative to external $\text{BF}_3\cdot\text{OEt}_2$) suggesting that the basic closed polyhedral ruthenacarborane structure was retained in the phosphine metathesis reaction. The ^1H NMR spectra of IIc,d showed two singlets due to two nonequivalent cage methyl groups, while those of IIa,b contained only one carboranyl C–H singlet, the other carboranyl C–H signal presumably being obscured by the aromatic resonances in the τ 2.7–3.2 range. This notion is supported by the $^{13}\text{C}\{^1\text{H}\}$ NMR spectrum of IIb, which exhibited two broad singlets (ca. 50 Hz half-widths) at 106.3 and

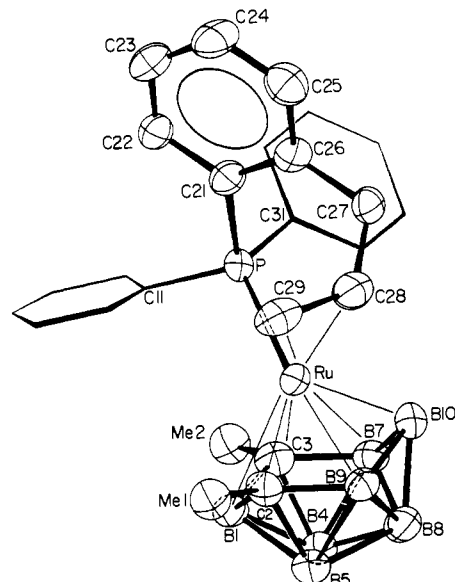


Figure 2. Structure of $[\text{hyper-closo-2,3-(CH}_3)_2\text{-6-(CH}_2)_2\text{-CHCH}_2\text{C}_6\text{H}_4\text{Ph}_2\text{P}]\text{-6,2,3-RuC}_2\text{B}_7\text{H}_7$ (IIc) and the numbering system employed. Atoms are shown as 50% probability ellipsoids. For the two phenyl rings, only the positions are indicated, and all hydrogen atoms have been removed for clarity.

122.2 ppm due to the two carboranyl carbon atoms. The other complexes either showed only one cage-carbon resonance (the second resonance is presumably buried under the aromatic carbon peaks) or were not sufficiently soluble to yield observable cage-carbon peaks. Cage-bonded methyl signals were not observed in the ^{13}C NMR spectra of IIc,d and may be too broad to detect at ambient temperature.^{18,19}

The spectral data presented for IIa–g are consistent with the alkenylphosphines acting as bidentate ligands. Since complexes IIa–g are electronically and somewhat coordinatively unsaturated, the two alkenyl groups of the ligand di(but-3-enyl)phenylphosphine could conceivably coordinate to the ruthenium atom.²⁰ However, the infrared, ^1H , and ^{13}C NMR spectra of IIg showed the presence of both free and coordinated butenyl side chains. The ^1H NMR spectrum was essentially temperature invariant over the range -50 to 40°C , ruling out an equilibrium between free and coordinated alkene.²¹ Steric hindrance and/or the additional metal–cage bonding interactions may prevent both butenyl side chains from bonding to the ruthenium atom simultaneously.

Complexes IIa–g were air stable in the solid state, but decomposed slowly in air-saturated solutions. They did not react with hydrogen (1 atm) or dry hydrogen chloride and complex IIa was an ineffective catalyst for alkene hydrogenation under mild conditions. No reduction of the alkenyl side chain^{21,22} of IIa was discernible even after several days in benzene solution under 1 atm pressure of hydrogen.

Treatment of IIb with carbon monoxide rapidly produced a yellow complex with empirical formula $[\text{Ru}(\text{CO})_2(\text{L})(\text{C}_2\text{B}_7\text{H}_9)]$ (IIIa, $\text{L} = \text{AP}$). The ^1H NMR spectrum of IIIa indicated that the allyl moiety is not coordinated to the metal atom. The carboranyl C–H resonances were not located, but the ^{11}B NMR spectrum of IIIa was almost identical with that of the complex $[\text{closo-6,6-(CO)}_2\text{-6-PPh}_3\text{-6,2,3-RuC}_2\text{B}_7\text{H}_9]$,⁴ suggesting that the two Ru^{II} complexes are isostructural.

Complex IIIa and its PPh_3 analogue are isoelectronic with $[\text{H}(\text{PPh}_3)_2\text{MC}_2\text{B}_7\text{H}_9]$ ($\text{M} = \text{Rh, Ir}$)⁴ and $[(\eta^5\text{-C}_5\text{H}_5)\text{Co}_2\text{C}_2\text{B}_6\text{H}_8]$,²³ and they presumably possess bicapped square

(11) M. A. Bennett, E. J. Hahn, and R. N. Johnson, *J. Organomet. Chem.*, **124**, 189 (1977).

(12) P. E. Garrou, J. L. S. Curtis, and G. E. Hartwell, *Inorg. Chem.*, **15**, 3094 (1976).

(13) M. A. Bennett, R. N. Johnson, and I. B. Tomkins, *J. Am. Chem. Soc.*, **96**, 61 (1974); M. A. Bennett and I. B. Tomkins, *J. Organomet. Chem.*, **51**, 289 (1973).

(14) M. A. Bennett, W. R. Kneen, and R. S. Nyholm, *Inorg. Chem.*, **7**, 552 (1968).

(15) M. A. Bennett, R. N. Johnson, and I. B. Tomkins, *Inorg. Chem.*, **13**, 346 (1974); **14**, 1908 (1975).

(16) P. W. Clark and G. E. Hartwell, *Inorg. Chem.*, **9**, 1948 (1970); *J. Organomet. Chem.*, **97**, 117 (1975); P. E. Garrou and G. E. Hartwell, *ibid.*, **55**, 331 (1973); **71**, 443 (1974).

(17) P. W. Clark and A. J. Jones, *J. Organomet. Chem.*, **122**, C41 (1976); P. W. Clark, P. Hanisch, and A. J. Jones, *Inorg. Chem.*, **18**, 2067 (1979).

(18) H. Beall and C. H. Bushweller, *Chem. Rev.*, **73**, 465 (1973).

(19) T. J. Marks and L. A. Shimp, *J. Am. Chem. Soc.*, **94**, 1452 (1972).

(20) P. W. Clark and G. E. Hartwell, *J. Organomet. Chem.*, **96**, 451 (1975).

(21) P. W. Clark and G. E. Hartwell, *J. Organomet. Chem.*, **102**, 387 (1975).

(22) G. E. Hartwell and P. W. Clark, *Chem. Commun.*, 1115 (1970).

antiprismatic structures, consistent with their formulation as saturated, ten-vertex *closo* polyhedra.²⁴ Complexes IIa-g and [(PPh₃)₂RuC₂B₇H₉],⁴ however, are unsaturated complexes, all of which exhibit a low-field ¹¹B NMR resonance at about 105 ppm and are isoelectronic with [(η⁵-C₅H₅)Fe]₂C₂B₆H₈, the structure of which has been determined.¹⁰ Nishimura has recently proposed²⁵ that the structure of [(η⁵-C₅H₅)Fe]₂C₂B₆H₈ can be rationalized in terms of a "hyperpolyhedral" metal-metal bond between the two 17e⁻ Fe^{III} centers of the cluster. In order to resolve this question by determining if an isoelectronic, unsaturated, monometallic ten-vertex cluster is, in fact, isostructural, an X-ray diffraction study of II d was undertaken.

Molecular Structure of [hyper-*closo*-2,3-(CH₃)₂-6-(CH₂=CHCH₂C₆H₄Ph₂P)-6,2,3-RuC₂B₇H₇] (II d). Intramolecular distances and their estimated standard deviations are listed in Table VI. Average bond lengths are collected in Table VII. Bond angles and their associated estimated standard deviations are listed in Table VIII. The structure of [2,3-(CH₃)₂-6-(CH₂=CHCH₂C₆H₄Ph₂P)-6,2,3-RuC₂B₇H₇] is shown in Figure 2, together with the numbering system employed.

The structure of this compound may be described in terms of a C₂B₇H₇Me₂ fragment of arachno geometry which occupies 9 vertices of an 11-vertex octadecahedron. The ruthenium atom occupies a position between the two empty vertices and is bound to the four boron atoms and two carbon atoms of the chair-shaped six-atom open face. The ruthenium atom is thus bound to B(10), B(9), B(7), C(2), C(3), and B(1) of the carborane cage and to P, C(28), and C(29) of the (*o*-allylphenyl)diphenylphosphine ligand. The polyhedral carbon atoms occupy positions 2 and 3 in the fragment and are formally five coordinate. The structure of [6,6-(PPh₃)₂-6,2,3-RuC₂B₇H₉]⁴ is probably similar with the ruthenium atom bonded to all six atoms in the open face (*vide infra*).

The ruthenium to cage distances can be compared to those in [2,2-(PPh₃)₂-2,2-H₂-2,1,7-RuC₂B₉H₁₁], which range from 2.22 (2) to 2.32 (2) Å for the five atoms of the carborane open face.² However, in the title compound, Ru-B distances involve bonds to boron atoms of different coordination numbers; Ru to six-coordinate boron B(7), B(9), and B(1) are 2.466 (5), 2.340 (5), and 2.488 (5) Å, respectively, and Ru to five-coordinate B(10) is 2.023 (5) Å. A similar change in Fe-B bond lengths is noted in a compound with comparable cage geometry, [hyper-*closo*-1,6-(η⁵-C₅H₅)₂-1,6,2,3-Fe₂C₂B₆H₈].¹⁰

As expected, the polyhedral carbon atoms occupy nonadjacent positions in this compound; they occupy two of the three low-coordinate positions and are related by a noncrystallographic mirror plane through Ru, B(10), B(8), and B(1). Variations from mirror symmetry are within three standard deviations in related bond distances with the exception of B(1)-C(3) and B(1)-C(2), Ru(6)-C(2) and Ru(6)-C(3), and Ru(6)-B(7) and Ru(6)-B(9). Two of these exceptions can be explained by trans influence.²⁶ The phosphorus atom is trans to B(9) and C(28)=C(29) is trans to C(3). Ru-C(3) is significantly longer than Ru-C(2) and Ru-B(9) is significantly shorter than Ru-B(7).

Unlike [1,6-(η⁵-C₅H₅)₂-1,6,2,3-Fe₂C₂B₆H₈], boron-boron distances and carbon-boron distances within the polyhedron do not reflect the coordination of the various atoms; the shortest boron-boron distance, B(4)-B(5) = 1.743 Å, is between two six-coordinate boron atoms, and the longest distances, B(1)-B(4), B(1)-B(5), and B(8)-B(9), 1.814, 1.820, and 1.814 Å, respectively, are also between two six-coordinate boron atoms.

In general, the bond lengths and angles within the C₂B₇ fragment correlate well with the analogous bonds in *arachno*-C₂B₇H₁₁Me₂.²⁷ The largest deviation is found for B(7)-C(3) and

B(9)-C(2). The corresponding distances in the arachno compound are 0.13 Å longer than those in the metallocarborane.

B(9), C(3), P, and the midpoint of C(28)=C(29) are in a square-planar conformation about Ru and C(28)=C(29) is nearly perpendicular to this plane. The Ru-P distance of 2.418 (1) Å is within the range of distances found for ruthenium bonded to phosphines, but is longer than those found in [2,2-(PPh₃)₂-2,2-(H₂)-2,1,7-RuC₂B₉H₁₁] (2.342 (4) and 2.301 (4) Å).² The longer bond in the title compound may be due to the bulky phosphine ligand with its allyl group. The Ru-C distances of 2.167 (4) and 2.191 (4) Å are well within the range of distances for Ru π bonded to an alkene.

Angles and distances involving the phosphorus atom are unexceptional. Although the phenyl ring of the *o*-allylphenyl moiety is planar, the dihedral angle C(27)-C(26)-C(21)-P is 4.4° and C(27), C(28), H(28), C(29), H(291), and H(292) are not coplanar. The linkage C(27)-C(28) is a normal single bond (1.5306 (6) Å) and the distance C(28)-C(29) (1.406 (7) Å) is within the range for π-bonded C=C distances. The distance of 1.498 (6) Å for C(26)-C(27) and distances and angles in the phenyl ring are not unusual.

The only intermolecular distance less than 2.5 Å is between H(292) and H(513) and is 2.44 Å. Only two nonhydrogen-hydrogen intermolecular distances are less than 3.0 Å and they are between phenyl carbon atoms and a phenyl hydrogen atom and a methyl hydrogen atom, respectively; each distance is 2.96 Å.

The polyhedral geometry of the title compound is significantly different from the bicapped square antiprism found for ten-vertex *closo*-borane species such as (B₁₀H₁₀)²⁻²⁸ and [(C₅H₅)₂Co₂C₂B₆H₆]²³ but is very similar to [(C₅H₅)₂Fe₂C₂B₆H₈]¹⁰ and does adopt a fully triangulated closed polyhedral structure. If the title compound was constrained to have the bicapped square antiprism form, a new bond would be needed between C(2) and C(3) and the Ru-B(1) bond would be broken. Then B(1) would be in a lower coordinate position and C(2) and C(3) would be located in six-coordinate positions.

The structures of the two hyper-*closo* ten-vertex metallocarboranes mentioned above also do not correspond to the predicted capping of the *closo* nine-vertex tricapped trigonal prism²⁹⁻³¹ but are instead a result of completely capping the six-membered open face of the arachno C₂B₇ fragment, presumably to compensate for the electronic unsaturation of the metal center.

Synthesis, Reactivity, and Variable Temperature Multinuclear FT NMR Studies of Closo Ruthenacarboranes. Complex [6,6-(PPh₃)₂-6,2,3-RuC₂B₇H₉] (Ia) reacted with MBP and DBP to produce yellow complexes with empirical formulas [RuL₂C₂B₇H₉] (IVa,b, L = MBP and DBP, respectively). The infrared spectra of IVa,b in the solid state contained both free and coordinated butenyl absorptions.¹² Solutions of IVa in toluene or dichloromethane were red at or above room temperature and the solution infrared spectrum in dichloromethane at 22 °C exhibited two additional peaks assignable to a coordinated butenyl side chain at 1325 and 1285 cm⁻¹ along with those at 1630 (free), 1300, and 1250 cm⁻¹ (coordinated) observed in the solid-state spectrum.³⁵

Complex IVb did not yield red solutions until the temperature was above about 60 °C. As the ligand cone angle³⁶ of MBP (140°) is larger than that of DBP (135°) it was presumed that phosphine

(23) E. L. Hoel, C. E. Strouse, and M. F. Hawthorne, *Inorg. Chem.*, **13**, 1388 (1974).

(24) K. Wade, *Prog. Inorg. Chem. Radiochem.*, **18**, 1 (1976).

(25) E. Nishimura, *J. Chem. Soc., Chem. Commun.*, 858 (1979).

(26) A. J. Welch, *J. Chem. Soc., Dalton Trans.*, 1473 (1976); W. E. Carroll, M. Green, F. G. A. Stone, and A. J. Welch, *ibid.*, 2263 (1975).

(27) D. Voet and W. N. Lipscomb, *Inorg. Chem.*, **6**, 113 (1967).

(28) R. D. Dobrott and W. N. Lipscomb, *J. Chem. Phys.*, **37**, 1779 (1962).
(29) R. Mason, K. M. Thomas, and D. M. P. Mingos, *J. Am. Chem. Soc.*, **95**, 3802 (1973).

(30) C. R. Eady, B. F. G. Johnson, and J. Lewis, *J. Chem. Soc., Dalton Trans.*, 2606 (1975).

(31) J. R. Pipal and R. N. Grimes, *Inorg. Chem.*, **16**, 3255 (1977), and references cited therein.

(32) H. M. Colquhoun, T. J. Greenhough, and M. G. H. Wallbridge, *J. Chem. Soc., Chem. Commun.*, 499 (1976); *J. Chem. Soc., Dalton Trans.*, 303 (1978); 619 (1979).

(33) D. M. P. Mingos, *J. Chem. Soc., Dalton Trans.*, 602 (1978).

(34) D. M. P. Mingos, M. I. Forsyth, and A. J. Welch, *J. Chem. Soc., Chem. Commun.*, 605 (1977).

(35) The band I absorption at ca. 1500 cm⁻¹ is presumably obscured by phenyl ring absorptions (see ref 12 and 21).

(36) C. A. Tolman, C. W. Seidel, and L. W. Gosser, *J. Am. Chem. Soc.*, **96**, 53 (1974); C. A. Tolman, *ibid.*, **92**, 2956 (1970).

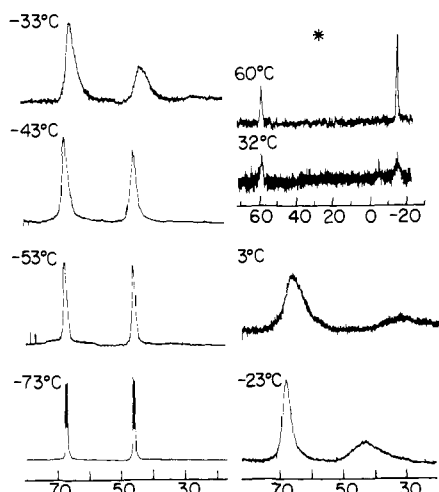


Figure 3. $^{31}\text{P}\{^1\text{H}\}$ FT NMR spectra of $[\text{closor-Ru}(\text{MBP})_2\text{C}_2\text{B}_7\text{H}_9]$ (IVa) in 20% $\text{CD}_2\text{Cl}_2/\text{CH}_2\text{Cl}_2$. The spectrum marked by an asterisk was recorded in 10% $\text{C}_6\text{D}_6/\text{C}_6\text{H}_5\text{CH}_3$. Scale is in parts per million downfield from D_3PO_4 .

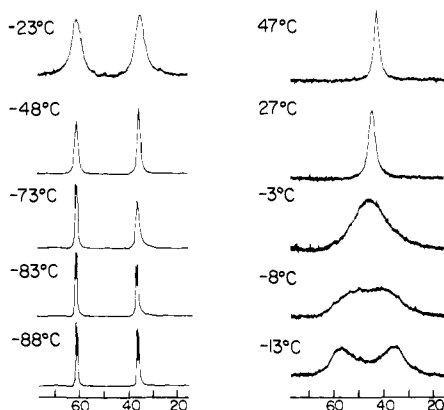


Figure 4. $^{31}\text{P}\{^1\text{H}\}$ FT NMR spectra of $[\text{closor-Ru}(\text{DBP})_2\text{C}_2\text{B}_7\text{H}_9]$ (IVb) in 20% $\text{CD}_2\text{Cl}_2/\text{CH}_2\text{Cl}_2$. Scale is in parts per million downfield from D_3PO_4 .

ligand dissociation occurs to yield the unsaturated, red [*hyper-closor*- $\text{LRuC}_2\text{B}_7\text{H}_9$] species. This proposal was supported by the observation of a low-field ^{11}B NMR resonance at 107.5 ppm in a dichloromethane- d_2 solution of IVa at 44 °C, which was absent at -40 °C. In addition, while treatment of IVb with carbon monoxide yielded $[\text{closor}(\text{CO})\text{L}_2\text{RuC}_2\text{B}_7\text{H}_9]$ in high yield, the yield of the analogous monocarbonyl complex of IVa decreased with increasing temperature, owing to the formation of the dicarbonyl complex $[\text{closor}(\text{CO})_2\text{LRuC}_2\text{B}_7\text{H}_9]$ (vide infra).

The variable temperature $^{31}\text{P}\{^1\text{H}\}$ FT NMR spectrum of IVa in dichloromethane shown in Figure 3 indicated that the $[\text{closor-L}_2\text{RuC}_2\text{B}_7\text{H}_9]$ species which predominates at low temperatures is itself fluxional. At -73 °C the spectrum consisted of a doublet for the chelated alkenylphosphine ligand^{12,37} at 68.5 ppm ($^2J_{\text{P-P}} = 32$ Hz) and a doublet for the unidentate phosphine ligand at 47.2 ppm. As the temperature was raised, these resonances broadened, but, before coalescence was attained, phosphine dissociation started to occur, as evidenced by the change in chemical shift of the unidentate phosphine ligand toward the free ligand limit. The spectrum at 60 °C in 10% C_6D_6 - $\text{C}_6\text{H}_5\text{CH}_3$ represented the high-temperature limit and exhibited a singlet at 49.8 ppm for the [*hyper-closor*- $\text{LRuC}_2\text{B}_7\text{H}_9$] species and a singlet at -15 ppm for the free alkenylphosphine ligand.⁸ The presence of two exchange processes was more evident in the variable temperature $^{31}\text{P}\{^1\text{H}\}$ FT NMR spectra of IVb in dichloromethane, as the temperature domains for the two processes were not overlapping. Thus, at -8 °C, coalescence of the two inequivalent phosphorus

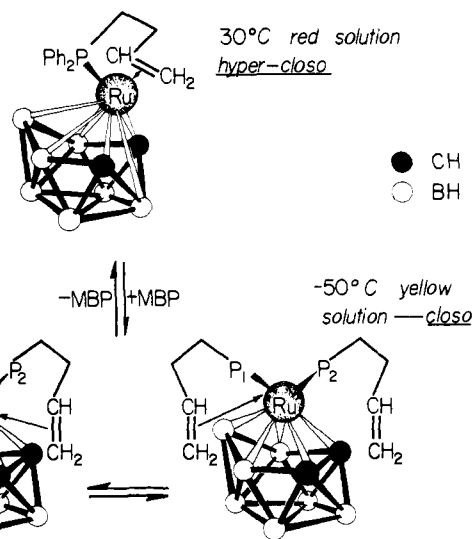


Figure 5. Proposed dynamic processes for $[\text{closor-Ru}(\text{MBP})_2\text{C}_2\text{B}_7\text{H}_9]$ (IVa).

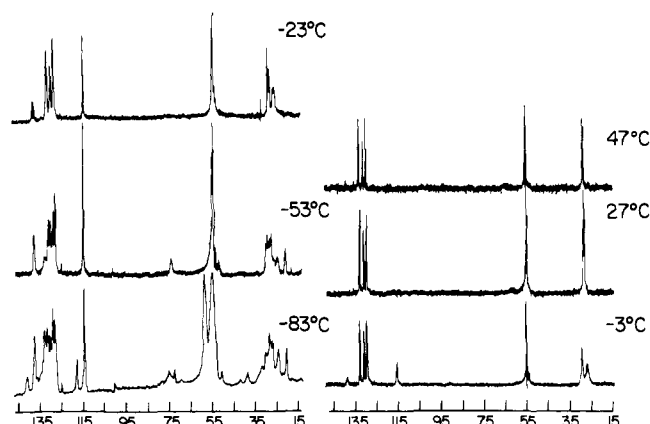


Figure 6. $^{13}\text{C}\{^1\text{H}\}$ FT NMR spectra of $[\text{closor-Ru}(\text{DBP})_2\text{C}_2\text{B}_7\text{H}_9]$ (IVb) in 20% $\text{CD}_2\text{Cl}_2/\text{CH}_2\text{Cl}_2$ (extra solvent peak at -83 °C is due to small amounts of solid $\text{CD}_2\text{Cl}_2/\text{CH}_2\text{Cl}_2$).

nuclei occurred cleanly and the change in chemical shift of the unidentate phosphine ligand did not begin until above 27 °C (Figure 4).

The variable temperature ^1H and $^{13}\text{C}\{^1\text{H}\}$ FT NMR spectra of IVa were also complicated owing to the overlap of the temperature domains of the two dynamic processes. At -78 °C the $^{13}\text{C}\{^1\text{H}\}$ FT NMR spectrum in dichloromethane exhibited free alkenyl carbons at 138.4 and 115.3 ppm, coordinated alkenyl carbons at 79.3 and 58.5 ppm, and carboranyl carbons at 72.7 and 41.2 ppm.³⁸ Broad, free alkenyl carbon resonances were observed at -23 °C, and at 27 °C the only resonances observed were due to exchange-averaged phenyl and methylene carbons of the alkenylphosphine ligand. The ^1H FT NMR spectrum of IVa in dichloromethane- d_2 at -68 °C consisted of three broad resonances at τ 5.39, 5.78, and 6.11, in addition to three resonances at τ 4.34, 5.09, and 5.16 which can be assigned to the coordinated and free alkenyl protons of butenyl side chains, respectively.¹⁶ At -38 °C these signals broadened and at 33 °C only one set of three alkenyl protons was observed, suggesting that the low-temperature exchange process is due to exchange of free and coordinated butenyl side chains,²¹ as depicted in Figure 5.

The variable temperature ^1H and $^{13}\text{C}\{^1\text{H}\}$ FT NMR spectra of IVb in dichloromethane were more informative, although the presence of three inequivalent butenyl side chains at the low-temperature limit led to overlapping resonances and precluded

(37) P. E. Garrou, *Inorg. Chem.*, **14**, 1435 (1975).

(38) The carboranyl carbon and carboranyl C-H proton resonances for IVa,b were only observed at low temperatures, presumably owing to the fluxional processes which occur at higher temperatures.

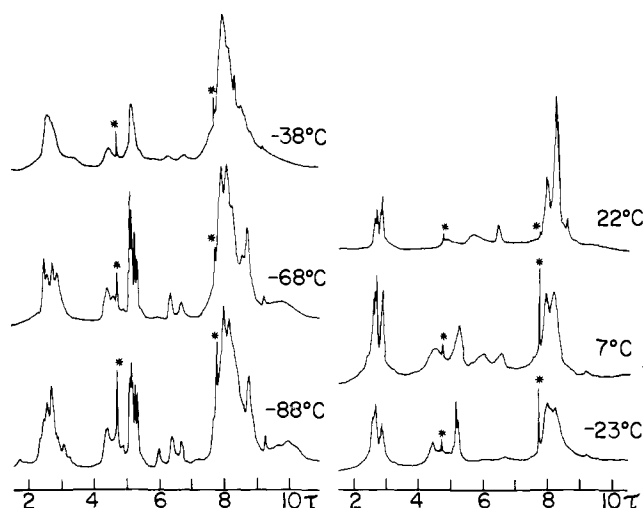


Figure 7. ^1H FT NMR spectra of IVb in CD_2Cl_2 . Resonances marked by asterisks are due to residual CH_2Cl_2 and toluene of crystallization.

complete spectral assignments. The $^{13}\text{C}\{^1\text{H}\}$ FT NMR spectra are shown in Figure 6.

At -83°C three sets of alkenyl carbons were observed at 142.3 and 119.2 (C_2' and C_1'), 138.5 and 115.6 (C_2 and C_1), and 74.8 and 52.5 (coordinated C_2' and C_1'), where the primed carbons refer to those butenyl side chains attached to the chelating phosphine ligand. The carboranyl carbons were observed at 75.9 and 39.2 ppm.³⁸ At -23°C only the C_1 and C_2 alkenyl carbon resonances were observed and at 27°C , again, only the exchange-averaged phenyl and methylene carbon resonances of the alkenylphosphine ligand were present. The ^1H FT NMR spectra of IVb in dichloromethane- d_2 are presented in Figure 7. At -88°C two sets of three free alkenyl proton resonances were observed at τ 4.41, 4.60 (H_3 and H_3'), 5.15, and 5.31 (H_1 , H_2 , H_1' and H_2' , overlapping), in addition to three coordinated alkenyl proton resonances at τ 6.00, 6.39, and 6.68. At 7°C two overlapping sets of three alkenyl proton resonances were present, while at 22°C only three alkenyl proton resonances were observed. It appears, then, from the $^{31}\text{P}\{^1\text{H}\}$, $^{13}\text{C}\{^1\text{H}\}$, and ^1H FT NMR spectral data, that there are, in fact, two low-temperature exchange processes occurring for IVb in solution. The first involves exchange of one butenyl side chain on each phosphine ligand between free and metal-coordinated sites, yielding equivalent phosphine ligands, one set of alkenyl carbon resonances due to the two nonfluxional butenyl side chains and two sets of alkenyl proton resonances due to the two nonfluxional butenyl side chains and the two exchange-averaged butenyl side chains. The second process involves exchange of all four butenyl side chains, yielding equivalent phosphine ligands, one set of exchange-averaged alkenyl protons, and no observed alkenyl carbon resonances. The activation energy (ΔG^\ddagger) for the exchange of the first two butenyl side chains is easily obtained from the $^{31}\text{P}\{^1\text{H}\}$ FT NMR spectra and is found to be 10.0 ± 0.5 kcal/mol.³⁹ The second process may be due to the onset of rotation about the ruthenium-phosphorus bond which would interchange the two butenyl side chains on each phosphine ligand, thus enabling all four butenyl side chains to exchange between free and coordinated sites.

The $^{11}\text{B}\{^1\text{H}\}$ FT NMR of IVb in dichloromethane- d_2 at -71°C resembled that of IVa at -40°C and illustrated the asymmetry induced in the carborane ligand when the phosphine ligands become inequivalent.

Complexes IVa,b reacted with carbon monoxide to form the yellow complexes [*closo*-6-CO-6,6- L_2 -6,2,3- $\text{RuC}_2\text{B}_7\text{H}_9$] (IVa,b, $\text{L} = \text{MBP}$ or DBP). The infrared spectra of IVa,b included ν_{CO} absorptions at 1932 and 1930 cm^{-1} and $\nu_{\text{C}=\text{C}}$ (uncoordinated) at 1628 and 1632 cm^{-1} , respectively. The ^1H NMR spectra in dichloromethane- d_2 contained alkenyl proton resonances due to

(39) This value agrees well with the more approximate values obtained from the $^{13}\text{C}\{^1\text{H}\}$ and ^1H FT NMR spectra for the same process.

uncoordinated butenyl side chains and exhibited no temperature-dependent behavior.⁴⁰ The presence of a mirror plane was indicated by the $^{11}\text{B}\{^1\text{H}\}$ and $^{31}\text{P}\{^1\text{H}\}$ NMR spectral data suggesting that the carboranyl cage mirror plane bisects the P-Rh-P angle in a static structure or, alternatively, that the $\{\text{RhP}_2\text{CO}\}$ vertex is rapidly rotating about the five-membered face of the carboranyl ligand as has been proposed for [*closo*- $\{\text{P}(\text{C}_2\text{H}_5)_3\}_3\text{RuC}_2\text{B}_7\text{H}_9$] at -88°C .⁴

The carbonylation of IVa produced Va in quantitative yield when monitored by $^{31}\text{P}\{^1\text{H}\}$ FT NMR at -78°C . At temperatures above 25°C , however, the carbonylation of IVa produced two additional singlet resonances at -15.3 and 45.4 ppm which were assigned to free but-3-enyldiphenylphosphine and to [*closo*-6,6-(CO) $_2$ -6- L -6,2,3- $\text{RuC}_2\text{B}_7\text{H}_9$] (IIIb, $\text{L} = \text{MPB}$), respectively. The infrared spectrum of IIIb in the 2100–1900- cm^{-1} region was very similar to that of the analogous complex, IIIa.

Conclusions

Reactions of [*hyper-closo*-2- R^1 -3- R^2 -6,6-(PPh_3) $_2$ -6,2,3- $\text{RuC}_2\text{B}_7\text{H}_9$] (I) with SP ($\text{R}^{1,2} = \text{H}, \text{CH}_3$; $\text{R}^1 = \text{H}$; $\text{R}^2 = \text{Ph}$), AP ($\text{R}^{1,2} = \text{H}, \text{CH}_3$), MBP, and DBP ($\text{R}^{1,2} = \text{CH}_3$) yielded the unsaturated ruthenacarborane complexes [*hyper-closo*- $\text{RuL}(\text{C}_2\text{B}_7\text{H}_7\text{R}^2)$] (IIa–g), in which the alkenylphosphine (L) functions as a bidentate ligand. The molecular structure of II d ($\text{L} = \text{AP}$; $\text{R}^{1,2} = \text{CH}_3$) was determined by X-ray diffraction to be similar to that of [$(\eta^5\text{-C}_5\text{H}_5\text{Fe})_2\text{C}_2\text{B}_6\text{H}_8$]¹⁰ and represents a new structural class of ten-vertex metallocarboranes containing ten skeletal electron pairs. The term “hyper-closo” has been adopted to describe this structural class of which [$(\eta^5\text{-C}_5\text{H}_5)_3\text{Co}_3\text{B}_4\text{H}_4$],³¹ [$(\eta^5\text{-C}_5\text{H}_5)\text{CoFe}(\text{CH}_3)_4\text{C}_4\text{B}_8\text{H}_8$],⁴¹ and [$\text{EFe}(\text{CH}_3)_4\text{C}_4\text{B}_8\text{H}_8$]⁴¹ ($\text{E} = \text{Sn}, \text{Ge}$) are also members, in order to differentiate these species from undistorted, unsaturated metallocarboranes, in which the electronic unsaturation is presumably largely metal based. Studies are now underway in this laboratory to isolate and determine the molecular structure of 12- and 11-vertex hyper-closo metallocarboranes in order to elucidate the nature of the polyhedral distortions induced by the unsaturated metal vertices.

Reactions of [*hyper-closo*-6,6-(PPh_3) $_2$ -6,2,3- $\text{RuC}_2\text{B}_7\text{H}_9$] with MBP and DBP yielded the saturated ruthenacarborane complexes [*closo*- $\text{RuL}_2(\text{C}_2\text{B}_7\text{H}_9)$] (IVa,b). A variable temperature multinuclear FT NMR study of IVa,b indicated that the complexes undergo butenyl side-chain exchange in solution at lower temperatures and undergo *closo*–*hyper-closo* equilibria with concomitant polyhedral rearrangement at higher temperatures. This facile rearrangement demonstrates the remarkable mobility of transition-metal vertices in cluster complexes and the flexibility of carborane cages in accommodating both electronic and coordinative unsaturation in the transition-metal vertex.

Several interesting metallocarboranes containing carboranyl cage-bonded alkenyl side chains have recently been prepared in this laboratory and the chemistry of these catalytically active species is currently under investigation.⁴²

Experimental Section

Crystal Structure. Crystals of II d suitable for X-ray studies were obtained as black needles from CH_2Cl_2 /pentane. A preliminary examination of several crystals by means of oscillation and Weissenberg photographs showed them to have monoclinic symmetry and systematic absences $0k0$, $k = 2n + 1$, and $h0l$, $l = 2n + 1$, space group $P2_1/c$.⁴³ The specimen selected for data collection was bounded by $\{102\}$, $\{010\}$, $\{110\}$, and $\{1\bar{1}0\}$. Crystal dimensions normal to these faces were 0.20, 0.16, 0.19, and 0.075 mm, respectively. The crystal was mounted on a Syntex P1 autodiffractometer equipped with a scintillation counter and a graphite monochromator. Lattice parameters, determined by a least-squares fit

(40) Compound IVa does appear to dissociate the MBP ligand at about 60°C but this process was not investigated in detail.

(41) W. M. Maxwell, K. Wong, and R. N. Grimes, *Inorg. Chem.*, **16**, 3094 (1977).

(42) M. S. Delaney, C. B. Knobler, R. G. Teller, and M. F. Hawthorne, *J. Am. Chem. Soc.*, to be submitted.

(43) “International Tables for X-ray Crystallography”, Vol. 1, Kynoch Press, Birmingham, England, 1962.

of 15 accurately centered high-angle reflections, were $a = 11.740$ (3) Å, $b = 15.185$ (5) Å, $c = 21.748$ (7) Å, and $\beta = 137.43$ (2)°. The density measured by flotation in aqueous potassium iodide was 1.36 (1) g cm⁻³, in good agreement with the calculated density of 1.368 g cm⁻³ based on $Z = 4$.

Intensity measurements were made with Mo K α radiation, scan rate of 2.0°/min from 1.25° below the K α_1 reflection to 1.25° above the K α_2 reflection. The background was counted for one-half of the scan time at each end of the scan range. Data were collected with a θ - 2θ scan technique to a limit of $2\theta = 55^\circ$. Three strong reflections were checked after each 97 intensity measurements and these showed only random variations consistent with their respective $\sigma(I)$ values. Of the 6052 unique reflections not excluded by the space group, 1884 for which $I < 3\sigma(I)$ were considered unobserved. The remaining 4168 reflections were used in the structure determination and refinement. All measured reflections were corrected for Lorentz and polarization effects and processed to give $|F_o|$ values as previously reported.⁴⁴ An absorption correction was applied ($\mu = 6.60$); maximum and minimum transmission factors were 0.9559 for $\bar{1}3018$ and 0.9479 for $\bar{1}1028$.

Determination and Refinement of the Structure. Trial positions for the ruthenium and phosphorus atoms were obtained from a three-dimensional Patterson summation. The other atoms, including hydrogen atoms, were located by means of difference Fourier maps. Refinement, without the contribution of hydrogen atoms to calculated structure factors, of positional and anisotropic thermal parameters of the ruthenium and phosphorus atoms and of positional and isotropic thermal parameters of all other nonhydrogen atoms converged to a conventional R^w index of 5.5% and a weighted index, R_w , of 7.5%. For reasons of economy, the two C₆H₅ moieties were then constrained to be rigid groups⁴⁶ containing C₆ hexagons of C-C = 1.39 and C-H = 1.0 Å. Maxima in the range of 0.5 ± 0.2 e Å⁻³ at positions close to those calculated for the remaining hydrogen atoms were found on a difference Fourier map. The two methyl groups were also constrained to be rigid groups containing an sp³ carbon atom and C-H = 1.0 Å. Positional and anisotropic thermal parameters of all nonhydrogen nongroup atoms, positional and isotropic thermal parameters of all carbon group atoms, and positional parameters of all nongroup hydrogen atoms were refined. Isotropic thermal parameters for all hydrogen atoms were assigned as follows: for all nongroup hydrogen atoms $B = 5.0$, for all phenyl group hydrogen atoms $B = 0.5$ plus the B value on the adjacent carbon atom, and for all methyl group hydrogen atoms $B = 1.0$ plus the B value on the adjacent carbon atom. The refinement converged at $R = 4.0\%$ and $R_w = 4.8\%$. In the final least-squares cycle, the largest shift in a positional or thermal parameter for a nonhydrogen atom was 0.4 σ . The final "goodness of fit" defined as $[\sum w(|F_o| - |F_c|)^2 / (N_o - N_v)]^{1/2}$ was 1.47. In this expression $N_o = 4168$, the number of observed reflections, and $N_v = 267$, the number of variable parameters. No maxima > 0.75 e Å⁻³ were found on a final difference Fourier map.

The final positional and thermal parameters are listed in Tables I-III. A listing of the root-mean-square amplitudes of vibration of the nonhydrogen nongroup atoms along the three principal axes of the vibrational ellipsoids, together with the corresponding B values, is given in Table IV.⁴⁷ A set of structure factors was calculated on the basis of the tabulated parameters and is available as Table V.⁴⁷ The atomic scattering factors were those given in Table 2.2A of ref 48 and the real and imaginary components of anomalous dispersion from Table 2.3.1 of ref 43 were applied to the scattering factors of ruthenium and phosphorus.

Synthesis of Metallocarboranes. Unless indicated otherwise, all operations were conducted under purified nitrogen or argon, using standard inert atmosphere techniques.⁴⁹

Infrared spectra were determined as mineral oil mulls or KBr pellets on a Perkin-Elmer 421 dual-grating spectrometer. ¹H NMR spectra were measured by using Varian A-60D and HA-100D spectrometers. ¹³C NMR spectra were recorded on a Varian CFT-20 spectrometer. The 80.5- and 111.8-MHz ¹¹B FT NMR spectra were obtained with an instrument designed and constructed by Professor F. A. L. Anet of this department. All other FT NMR spectra were recorded on a Bruker WP-200 spectrometer equipped with a B-UT-1000 variable temperature

(44) Experimental and computational procedures utilized in this investigation were similar to those reported in previous work. See K. P. Callahan, F. Y. Lo, C. E. Strouse, A. L. Sims, and M. F. Hawthorne, *Inorg. Chem.*, **13**, 2842 (1974).

(45) $R = [\sum |F_o| - |F_c|] / \sum |F_o|$; $R_w = [\sum w(|F_o| - |F_c|)^2 / \sum w|F_o|^2]^{1/2}$; $w = 1/(\sigma F)^2$. The function $\sum w(|F_o| - |F_c|)^2$ was minimized in least-squares refinement.

(46) C. Scheringer, *Acta Crystallogr.*, **16**, 546 (1963).

(47) See paragraph at end of paper regarding supplementary material.

(48) Reference 43, Vol. IV, 1974.

(49) D. F. Shriver, "The Manipulation of Air-Sensitive Compounds", McGraw-Hill, New York, 1969.

Table I. Atomic Positional Parameters in

atom	x	y	z
Ru	-0.088 32 (4) ^b	0.233 99 (2)	0.177 00 (2)
P	-0.156 48 (11)	0.235 07 (7)	0.041 55 (6)
B(1)	-0.1975 (6)	0.3612 (3)	0.1937 (3)
B(4)	-0.3551 (6)	0.2987 (4)	0.1727 (3)
B(5)	-0.1548 (6)	0.3089 (3)	0.2843 (3)
B(7)	-0.3555 (6)	0.2025 (4)	0.1242 (4)
B(8)	-0.2486 (7)	0.2009 (4)	0.2395 (4)
B(9)	-0.0303 (6)	0.2185 (3)	0.3050 (3)
B(10)	-0.1602 (6)	0.1430 (3)	0.2111 (3)
C(2)	-0.0176 (5)	0.3131 (3)	0.2798 (3)
C(3)	-0.3263 (5)	0.2968 (3)	0.1072 (3)
C(21)	0.0166 (5)	0.1999 (3)	0.0609 (3)
C(22)	0.0605 (5)	0.2452 (3)	0.0248 (3)
C(23)	0.1907 (6)	0.2151 (3)	0.0393 (3)
C(24)	0.2768 (6)	0.1394 (4)	0.0894 (4)
C(25)	0.2346 (6)	0.0944 (3)	0.1256 (4)
C(26)	0.1052 (5)	0.1233 (3)	0.1126 (3)
C(27)	0.0672 (6)	0.0757 (3)	0.1562 (4)
C(28)	0.0936 (5)	0.1316 (3)	0.2244 (3)
C(29)	0.1741 (5)	0.2140 (3)	0.2580 (3)
H(1) ^c	-0.199 (7)	0.431 (4)	0.184 (4)
H(4)	-0.466 (7)	0.322 (4)	0.150 (4)
H(5)	-0.119 (7)	0.345 (4)	0.341 (4)
H(7)	-0.470 (7)	0.164 (4)	0.068 (4)
H(8)	-0.295 (7)	0.162 (4)	0.259 (4)
H(9)	0.078 (7)	0.184 (4)	0.368 (4)
H(10)	-0.134 (7)	0.074 (4)	0.225 (4)
H(22)	0.001 (8)	0.299 (4)	-0.007 (4)
H(23)	0.221 (8)	0.242 (4)	0.015 (4)
H(24)	0.360 (7)	0.118 (4)	0.100 (4)
H(25)	0.292 (8)	0.044 (4)	0.162 (4)
H(271)	0.143 (7)	0.022 (4)	0.188 (4)
H(272)	-0.052 (8)	0.055 (4)	0.109 (4)
H(28)	0.121 (7)	0.097 (4)	0.274 (4)
H(291)	0.196 (8)	0.242 (4)	0.230 (4)
H(292)	0.231 (8)	0.225 (4)	0.316 (4)

^a Atomic positional parameters for atoms which have been treated as members of rigid groups are listed in Table II. ^b The numbers given in parentheses here and in succeeding tables are the estimated standard deviations in the least significant digits. ^c Hydrogen atoms are numbered according to the number of the atom to which they are bonded.

unit. ¹¹B and ³¹P chemical shifts were referenced to external BF₃·OEt₂ and D₃PO₄, respectively, with positive values assigned to low-field shifts, and all reported coupling constants are absolute values. All NMR solvents were vacuum distilled from P₂O₁₀ into the NMR sample tube prior to sealing under vacuum ($< 5 \times 10^{-5}$ torr). Mass spectra were obtained on an Associated Electrical Industries MS-9 spectrometer.

Melting points were determined in open capillaries and are uncorrected. Elemental analyses were performed by Schwarzkopf Microanalytical Laboratories, Woodside, N.Y.

The complex [*hyper-closo*-2-R¹-3-R²-6,6-(PPH₃)₂-6,2,3-RuC₂B₇H₉] was prepared by a previously described procedure.⁴ SP,⁶ AP,⁷ MBP,⁸ and DBP⁸ were prepared by literature methods. Toluene, benzene, and petroleum ether (30-60 °C) were distilled from calcium hydride. Other solvents were reagent grade and deoxygenated with bubbling nitrogen or argon immediately before use. All other chemicals were reagent grade and used as supplied.

Preparation of [*hyper-closo*-6-(SP)-6,2,3-RuC₂B₇H₉] (IIa). A toluene (2 mL) solution of [Ru(PPH₃)₂(C₂B₇H₉)] (0.101 g, 0.138 mmol) and SP (0.0875 g, 0.304 mmol) was stirred overnight at room temperature, yielding a deep blood-red solution. Pentane (10 mL) was gently layered above the toluene solution and the mixture was cooled to -15 °C for 3 days. The resulting red-brown crystals of [Ru(SP)(C₂B₇H₉)] (IIa, 0.049 g, 68%) were filtered off in air, washed with methanol and pentane, and vacuum dried, mp 193-197 °C. Anal. Calcd for C₂₂H₂₆B₇PRu: C, 53.04; H, 5.26; B, 15.19. Found: C, 53.10; H, 5.42; B, 15.36. ¹H NMR (100 MHz, CD₂Cl₂): τ 7.85 (dd { $J_{13} = 8.4$, $J_{P-H} = 1.3$ Hz}, H₁), 7.20 (d { $J_{23} = 11.9$, $J_{P-H} < 0.5$ Hz}, H₂), 4.87 (q { $J_{P-H} < 0.5$ Hz}, H₃), 3.96 (br s, carborane C-H). ¹³C{¹H} NMR (20.5 MHz, 20% CD₂Cl₂/CH₂Cl₂): 66.25 (s, C₁, $J_{C-H} = 152.5, 159.8$ Hz), 92.55 (s, C₂, $J_{C-H} = 158.8$ Hz), and 110.1 ppm (br s, carborane C { $W_{1/2} \approx 50$ Hz}). ¹¹B NMR (80.5 MHz, CD₂Cl₂): 106.8 (1), 18.9 (1), 5.59 (1), -3.75, -4.55,

Table II

A. Atomic Positional Parameters for Members of Rigid Groups in [2,3-(CH ₂ =CHCH ₂ C ₆ H ₄ Ph ₂ P)-6,2,3-RuC ₂ B ₇ H ₇]											
group	atom	x	y	z	group	atom	x	y	z		
phenyl 1	C(11)	-0.1902	0.3495	0.0058	phenyl 3	C(31)	-0.3302	0.1692	-0.0579		
	C(12)	-0.3348	0.3804	-0.0805		C(32)	-0.3778	0.1763	-0.1381		
	C(13)	-0.3540	0.4699	-0.0995		C(33)	-0.5033	0.1220	-0.2114		
	C(14)	-0.2285	0.5286	-0.0321		C(34)	-0.5813	0.0606	-0.2044		
	C(15)	-0.0839	0.4977	0.0543		C(35)	-0.5337	0.0536	-0.1242		
	C(16)	-0.0647	0.4082	0.0732		C(36)	-0.4081	0.1079	-0.0509		
	H(12)	-0.425	0.338	-0.129		H(32)	-0.322	0.220	-0.143		
	H(13)	-0.458	0.492	-0.162		H(33)	-0.538	0.127	-0.269		
	H(14)	-0.242	0.593	-0.046		H(34)	-0.672	0.022	-0.257		
	H(15)	0.006	0.540	0.103		H(35)	-0.590	0.009	-0.119		
	H(16)	0.039	0.386	0.135		H(36)	-0.374	0.103	0.007		
	methyl 1	C(41)	0.1430	0.3679		0.3493	methyl 2	C(51)	-0.4622	0.3372	0.0130
		H(411)	0.149	0.410		0.317		H(511)	-0.564	0.336	0.000
		H(412)	0.143	0.401		0.389		H(512)	-0.438	0.399	0.010
		H(413)	0.243	0.328		0.388		H(513)	-0.484	0.300	-0.033

B. Group Parameters for Rigid Groups ^a						
group	x, Å	y, Å	z, Å	φ, deg	θ, deg	ρ, deg
phenyl 1	-0.1902 (3)	0.3495 (1)	0.0058 (2)	-59.2 (3)	-110.1 (1)	-144.2 (3)
phenyl 3	-0.3302 (3)	0.1692 (2)	-0.0579 (2)	120.6 (1)	-147.8 (1)	-113.6 (1)
methyl 1	0.1429 (6)	0.3679 (3)	0.3493 (3)	138 (3)	-132 (3)	91 (4)
methyl 2	-0.4622 (6)	0.3372 (3)	0.0130 (3)	-81 (2)	172 (3)	-114 (3)

^a These parameters are defined in ref 46.

Table III. Atomic Thermal Parameters in [2,3-(CH₃)₂-6-(CH₂=CHCH₂C₆H₄Ph₂P)-6,2,3-RuC₂B₇H₇]^a

atom	β ₁₁	β ₂₂	β ₃₃	β ₁₂	β ₁₃	β ₂₃
Ru	802 (5)	255 (1)	239 (1)	7 (2)	310 (2)	20 (1)
P	866 (14)	226 (4)	265 (4)	-16 (7)	349 (7)	7 (4)
B(1)	1223 (80)	301 (24)	327 (23)	29 (33)	467 (38)	9 (18)
B(4)	1219 (81)	429 (25)	374 (24)	1 (36)	527 (40)	-29 (20)
B(5)	1339 (83)	350 (25)	344 (23)	-8 (36)	519 (40)	-17 (19)
B(7)	1075 (77)	423 (25)	405 (26)	-125 (36)	499 (41)	-86 (21)
B(8)	1497 (90)	376 (24)	408 (26)	-148 (38)	623 (44)	-56 (20)
B(9)	1320 (79)	326 (26)	305 (22)	10 (34)	483 (37)	24 (18)
B(10)	1409 (86)	272 (23)	411 (25)	-105 (34)	589 (43)	-28 (19)
C(2)	1141 (66)	293 (20)	276 (18)	-49 (28)	397 (31)	-19 (14)
C(3)	913 (62)	409 (21)	289 (19)	54 (28)	367 (31)	10 (16)
C(21)	923 (60)	271 (17)	316 (19)	-17 (25)	403 (30)	-13 (14)
C(22)	1176 (66)	348 (23)	312 (19)	-20 (28)	445 (32)	14 (15)
C(23)	1348 (74)	496 (28)	449 (24)	-69 (34)	653 (39)	6 (19)
C(24)	1394 (85)	616 (31)	555 (29)	155 (40)	725 (46)	54 (23)
C(25)	1704 (92)	413 (26)	576 (29)	303 (38)	778 (47)	136 (21)
C(26)	1299 (72)	303 (20)	415 (22)	74 (29)	576 (36)	27 (16)
C(27)	1858 (90)	291 (21)	591 (28)	248 (35)	879 (47)	149 (19)
C(28)	1396 (78)	377 (23)	426 (24)	321 (33)	610 (39)	161 (18)
C(29)	969 (67)	539 (30)	327 (21)	193 (33)	381 (34)	90 (19)

group	atom	B, Å ²	group	atom	B, Å ²
phenyl 1	C(11)	2.58 (7)	phenyl 3	C(31)	2.61 (7)
	C(12)	3.48 (8)		C(32)	3.48 (8)
	C(13)	4.66 (11)		C(33)	4.44 (10)
	C(14)	5.11 (11)		C(34)	4.38 (10)
	C(15)	4.75 (11)		C(35)	4.26 (10)
	C(16)	3.50 (8)		C(36)	3.37 (8)
methyl 1	C(41)	3.74 (9)	methyl 2	C(51)	3.97 (9)

^a All values of β have been multiplied by 10⁵. The anisotropic temperature factor expression is of the form exp[-(β₁₁h² + β₂₂k² + β₃₃l² + 2β₁₂hk + 2β₁₃hl + 2β₂₃kl)]. The hydrogen atoms were assigned fixed isotropic thermal parameters: all cage hydrogen atoms had B values fixed at 5.0 Å², all other hydrogen atoms which are not members of rigid groups also were assigned B = 5.0 Å², all methyl group hydrogen atoms were assigned B values 1.0 Å² greater than the B value on the adjacent carbon atom, and all phenyl group hydrogen atoms were assigned B values 0.5 Å² greater than those of the adjacent carbon atoms.

-5.94 (3, overlapping peaks), -8.82 ppm (1).

Analogous [RuL(C₂B₇H₇R¹R²)] complexes were prepared similarly by reactions of [2-R¹-3-R²-6,6-(PPh₃)₂-6,2,3-RuC₂B₇H₇] with the appropriate alkenylphosphine. [Ru(AP)(C₂B₇H₇)] (IIb): AP (0.208 g, 0.685 mmol), [Ru(PPh₃)₂(C₂B₇H₇)] (0.251 g, 0.342 mmol), 85% yield, mp 157-160 °C. Anal. Calcd for C₂₃H₂₈B₇PRu: C, 53.94; H, 5.51; B, 14.78; P, 6.05; Ru, 19.73. Found: C, 53.79; H, 5.65; B, 14.93; P, 6.28; Ru, 19.53. ¹H NMR (100 MHz, CD₂Cl₂): τ 8.37 (dd {J₁₃ = 7.8, J_{P-H1} = 2.5 Hz}, H₁), 7.53 (dd {J₂₃ = 13.0, J_{P-H2} ≈ 1 Hz}, H₂), 5.53 (m, H₃), 6.13 (m, CH₂), 4.88 (br s, carborane C-H). ¹³C{¹H} NMR (20.5 MHz,

20% CD₂Cl₂/CH₂Cl₂): 66.52 (s, C₁), 88.66 (d {⁴J_{P-C2} = 5.0 Hz}, C₂), 39.54 (d {³J_{P-C} = 14.0 Hz}, CH₂), 106.3 and 122.2 ppm (br s, carborane C). ¹¹B NMR (80.5 MHz, CD₂Cl₂): 108.4 (1), 15.0 (1), 4.80 (1), -5.18 (1), 7.01 (2), -10.3 (1) ppm. [Ru(SP)(C₂B₇H₇Me₂)] (IIc): SP (0.15 g, 0.52 mmol), [Ru(PPh₃)₂(C₂B₇H₇Me₂)] (0.206 g, 0.270 mmol). Anal. Calcd for C₂₄H₃₀B₇PRu: C, 54.78; H, 5.75; P, 5.88. Found: C, 55.61; H, 6.31; P, 5.65. ¹H NMR (100 MHz, CD₂Cl₂): τ 7.51 (dd {J₁₃ = 8.6, J_{P-H1} = 2.0 Hz}, H₁ (upfield half obscured by Me singlet)), 8.01 (dd {J₂₃ = 12.2, J_{P-H2} = 1.6 Hz}, H₂), 5.14 (q {J_{P-H3} < 0.5 Hz}, H₃), 7.53 and 8.77 (s, CH₃). ¹¹B NMR (CD₂Cl₂): 107.6 (1), 17.9 (1), 11.9 (1), -0.12 (1),

-2.21 (2), -9.56 ppm (1). [Ru(AP)(C₂B₇H₇Me₂)] (IIId): AP (0.091 g, 0.301 mmol), [Ru(PPh₃)₂(C₂B₇H₇Me₂)] (0.153 g, 0.201 mmol), 70% yield. Anal. Calcd for C₂₅H₃₂B₇PRu: C, 55.58; H, 5.97; P, 5.73. Found: C, 55.92; H, 6.07; P, 5.38. ¹H NMR (100 MHz, CD₂Cl₂): 7.52 (dd {J₁₂ = 3.5, J₁₃ = 7.5, J_{P-H} < 0.5 Hz}, H₁), 8.01 (dd {J₂₃ = 8.2, J_{P-H} < 0.5 Hz}, H₂), 5.58 (m, H₃), 6.14 (m, CH₂), 7.69 and 8.77 (s, CH₃). ¹³C{¹H} NMR (20% CD₂Cl₂/CH₂Cl₂): 55.73 (s, C₁), 88.76 (d {J_{P-C} = 4.1 Hz}, C₂), 39.49 ppm (d {J_{P-C} = 15.2 Hz}, CH₂). ¹¹B NMR (CD₂Cl₂): 108.0 (1), 19.2 (1), 14.6 (1), -2.06 (3), -11.0 ppm (1). [Ru(SP)(C₂B₇H₈Ph)] (IIe): SP (0.149 g, 0.517 mmol), [Ru(PPh₃)₂(C₂B₇H₈Ph)] (0.279 g, 0.344 mmol), 58% yield. Anal. Calcd for C₂₈H₃₀B₇PRu: C, 58.56; H, 5.26; P, 5.39. Found: C, 58.58; H, 5.42; P, 5.70. ¹H NMR (100 MHz, CD₂Cl₂): τ 8.55 (dt {J₁₂ ≈ 1, J₁₃ = 8.8, J_{P-H} ≈ 1 Hz}, H₁), 7.70 (dt {J₂₃ = 12.0, J_{P-H} ≈ 1 Hz}, H₂), 4.83 (q {J_{P-H} < 0.5 Hz}, H₃), 4.19 (br s, carborane C-H). ¹³C{¹H} NMR (20% CD₂Cl₂/CH₂Cl₂): 65.44 (s {J_{C-H} = 155, 162 Hz}, C₁), 92.35 (s {J_{C-H} = 159 Hz}, C₂), 104.2 ppm (br s, carborane C). ¹¹B NMR (CD₂Cl₂): 106.8 (1), 15.2 (1), 9.09 (1), -4.82 (3), -10.4 ppm (1). [Ru(MBP)(C₂B₇H₇Me₂)] (IIIf): MBP (0.21 g, 0.87 mmol), [Ru(PPh₃)₂(C₂B₇H₇Me₂)] (0.301 g, 0.395 mmol), 77.5% yield, mp 250–280 °C dec. Anal. Calcd for C₂₀H₃₀B₇PRu: C, 50.24; H, 6.32; P, 6.48. Found: C, 50.33; H, 6.55; P, 6.55. ¹H NMR (100 MHz, CD₂Cl₂): τ 7.87 (d {J₁₃ = 8.5 Hz}, H₁), ca. 7.3 (peak partially obscured by CH₂ resonances, H₂), 5.59 (m, H₃), 6.8–7.5 (m, CH₂), 7.61 and 8.42 (s, CH₃). ¹³C{¹H} NMR (20% CD₂Cl₂/CH₂Cl₂): 55.42 (s, C₁), 94.98 (d {J_{P-C} = 2.6 Hz}, C₂), 30.1–33.4 ppm (CH₂). ¹¹B NMR (CD₂Cl₂): 107.5 (1), 17.5 (1), 10.6 (1), 0.19 (1), -2.30 (1), -3.59 (1), -9.65 ppm (1). [Ru(DBP)(C₂B₇H₇Me₂)] (IIg): DBP (0.19 g, 0.87 mmol), [Ru(PPh₃)₂(C₂B₇H₇Me₂)] (0.302 g, 0.396 mmol), 56% yield, mp 119–130 °C dec. Anal. Calcd for C₁₈H₃₂B₇PRu: C, 47.39; H, 7.07; P, 6.79. Found: C, 47.46; H, 7.08; P, 6.79. ¹H NMR (100 MHz, CD₂Cl₂): τ ca. 8.0 and 7.2 (H₁ and H₂, respectively, peaks partially obscured by CH₂ resonances), 5.07 (m, H₃), 6.8–8.2 (m, CH₂), 7.66 and 8.30 (s, CH₃), 4.16 (m, uncoordinated H₃), 4.88 (m, uncoordinated H₁ and H₂). ¹³C NMR (20% CD₂Cl₂/CH₂Cl₂): 54.53 (s {J_{C-H} = 142.5, 165 Hz}, C₁), 94.65 (s {J_{C-H} = 156.5 Hz}, C₂), 23.2–32.8 (alkyl), 116.28 (d {J_{P-C} = 22.2 Hz}, uncoordinated C₁), 137.5 ppm (d {J_{P-C} = 14 Hz}, uncoordinated C₂). ¹¹B NMR (CD₂Cl₂): 106.8 (1), 17.2 (1), 9.73 (1), -0.11 (1), -2.30 (1), -4.48 (1), -9.85 ppm (1). Infrared spectrum (KBr): free ν_{C=C} at 1629 cm⁻¹.

Reaction of [6-(AP)-6,2,3-RuC₂B₇H₉] with Carbon Monoxide. A toluene (1 mL) solution of [Ru(AP)(C₂B₇H₉)] (54.0 mg, 0.105 mmol) was stirred under a carbon monoxide atmosphere, and the initial blood-red color turned yellow instantly. After 5 min petroleum ether (20 mL) was layered on top of the toluene, and the mixture was allowed to stand for 4 h undisturbed. The resulting yellow crystals were filtered in air, washed with petroleum ether and methanol, and recrystallized from dichloromethane/petroleum ether affording [closo-6,6-(CO)₂-6-AP-6,2,3-RuC₂B₇H₉] (IIIg, 27%), mp 172–176 °C. Anal. Calcd for C₂₅H₂₈B₇PO₂Ru: C, 52.84; H, 4.97; P, 5.45. Found: C, 53.06; H, 5.21; P, 4.97. ¹H NMR (100 MHz, CD₂Cl₂): τ 5.09 (m, H₁), 4.96 (m, H₂), 4.40 (m, H₃), and 6.62 (m, CH₂). ¹¹B{¹H} NMR (CD₂Cl₂): 1.40 (2), -9.33 (1), -20.4 and -23.2 ppm (4, overlapped peaks). Infrared spectrum (KBr): ν_{CO} at 2037 (s) and 1980 cm⁻¹ (s) and free ν_{C=C} at 1630 cm⁻¹.

Preparation of [closo-6,6-(MBP)₂-6,2,3-RuC₂B₇H₉] (IVa). To a stirred suspension of [Ru(PPh₃)₂(C₂B₇H₉)] (0.102 mg, 0.138 mmol) in toluene (2 mL) was added (but-3-enyl)diphenylphosphine (0.078 g, 0.32 mmol). The blue solution instantly turned red. After 15 min, pentane (60 mL) was layered above the toluene solution. After standing undisturbed overnight the mixture was cooled to -15 °C for 2 days, precipitating yellow crystals of [closo-6,6-(MBP)₂-6,2,3-RuC₂B₇H₉] (IVa, 0.066 g, 69%) which were filtered quickly in air, washed with methanol and petroleum ether, and vacuum dried, mp 115–126 °C dec (darkens at 100 °C). Anal. Calcd for C₃₃H₄₃B₇P₂Ru: C, 59.15; H, 6.28; P, 8.97. Found: C, 60.45; H, 6.56; P, 8.53.

¹H FT NMR (200.133 MHz, CD₂Cl₂, 33 °C): τ 2.60 (m, phenyl protons), 4.7, 6.3, 6.7 (br, alkenyl protons), and 7.58 (br, methylene protons). At -38 °C: τ 2.70 (br m, phenyl protons), 4.90 (br, alkenyl protons), and 7.65 (br, methylene protons). At -68 °C: 2.27, 2.56, 2.73, 2.90 (m, phenyl protons), 3.54, 4.88 (br s, carborane C-H protons), 4.34 (br, m, uncoordinated H₃), 5.09 (br s) and 5.16 (d, J₂₋₃ = 10 Hz) (uncoordinated H₁ and H₂, respectively), 5.39, 5.78, 6.11 (br, coordinated alkenyl protons), 7.23 and 8.17 (br m, methylene protons). ¹³C{¹H} FT NMR (50.32 MHz, 20% CD₂Cl₂/CH₂Cl₂, 22 °C): 133.7 (d, J_{P-C} = 13 Hz, ortho phenyl carbon), 131.3 (s, para carbon), 129.8 (d, J_{P-C} = 10 Hz, meta carbon) and 31.6 ppm (overlapping doublets, J_{P-C} = 18, J_{P-C} = 11 Hz, methylene carbons). At -23 °C: 138 (br, uncoordinated C₂), 134–129 (complex multiplet, phenyl carbons), 115 (br, uncoordinated C₁) and 28 ppm (br, methylene carbons). At -78 °C: 138.4 (d, J_{P-C} = 12 Hz, uncoordinated C₂), 133.4–127.8 (complex multiplet, phenyl carbons), 115.3 (s, uncoordinated C₁), 79.3 (s, coordinated C₂), 72.7 (br, carborane

carbon), 58.5 (s, coordinated C₁), 41.2 (br, carborane carbon), 35.4 (d, J_{P-C} = 25 Hz) and 29.8 (s) (methylene carbons of coordinated butenyl side chain), 27.5 (d, J_{P-C} = 20 Hz) and 23.2 ppm (s) (methylene carbons of uncoordinated butenyl side chain). ³¹P{¹H} FT NMR (81.02 MHz, 20% CD₂Cl₂/CH₂Cl₂, 60 °C): 59.8 (s) and -13.7 ppm (s). At 32 °C in 20% CD₂Cl₂/CH₂Cl₂: 60.3 and -14.0 ppm (br s, W_{1/2} ≈ 200 Hz). At -23 °C: 66.8 (br s, W_{1/2} ≈ 200 Hz) and 42.3 ppm (br s, W_{1/2} ≈ 650 Hz). At -73 °C: 68.5 (d, J_{P-P} = 32 Hz) and 47.2 ppm (d). ¹¹B{¹H} FT NMR (111.8 MHz, CD₂Cl₂, 44 °C): 107.5 (1), 17.3 (1), 2.5 (1), -5.0 (2), -6.5 (1), and -8.7 ppm (1). At -40 °C: 20.4 (2), -6.0 (2), and -23.2 ppm (3). Infrared spectrum (Nujol): 3045 (w), 3525 (s, br), 1941 (w), 1630 (m), 1578 (w), 1563 (w), 1424 (s), 1300 (w), 1250 (w), 1174 (w), 1149 (w), 1093 (m, sh), 1077 (m), 1053 (m, sh), 1019 (w), 980 (m, br), 933 (w), 897 (m), 886 (w), 786 (w), 738 (s), 692 cm⁻¹ (s). In CH₂Cl₂ solution: two additional weak bands at 1325 and 1285 cm⁻¹.

The complex [closo-6,6-(DBP)₂-6,2,3-RuC₂B₇H₉] (IVb) was synthesized from DBP (0.080 g, 0.367 mmol) and [Ru(PPh₃)₂(C₂B₇H₉)] (0.100 g, 0.136 mmol) in 2 mL of toluene and worked up as described above, yield 0.062 g (70%), mp 91–96 °C dec. Anal. Calcd for C₃₃H₃₅H₅B₇P₂Ru (IVb-0.5C₆H₅CH₃): C, 58.10; H, 7.47; P, 8.95. Found: C, 57.02; H, 7.39; P, 8.89. ¹H FT NMR (200.133 MHz, CD₂Cl₂, 22 °C): τ 2.66, 2.82 (m, phenyl protons), 4.82, 5.65, 6.42 (br, alkenyl protons), 7.92 and 8.17 (br, methylene protons). At 7 °C: τ 2.61, 2.85 (m, phenyl protons), 4.42, 5.17, 5.98, 6.55 (br, overlapping alkenyl proton resonances), 7.93 and 8.15 (br, methylene protons). At -88 °C: 2.57, 2.71 (m, phenyl protons), 3.07 (br, carborane C-H), 4.41 (br, uncoordinated H₃), 4.68 (br, uncoordinated H₃'), 4.90 (br, carborane C-H), 5.25 (complex multiplet, uncoordinated H₁, H₂, H₁', H₂'), 6.00, 6.39, 6.68 (br, coordinated H₁', H₂', H₃'), 7.99, 8.15, and 8.77 ppm (br, methylene protons). ¹³C{¹H} FT NMR (50.32 MHz, 20% CD₂Cl₂/CH₂Cl₂, 27 °C): 132.9 (d, J_{P-C} = 8 Hz, ortho phenyl carbon), 131.0 (s, para carbon), 129.6 (d, J_{P-C} = 8 Hz, meta carbon), and 28.5 ppm (overlapping doublet and singlet, J_{P-C} = 15 Hz, methylene carbons). At -23 °C: 138.7 (d, J_{P-C} = 12 Hz, uncoordinated C₂), 132.4, 130.7, 129.3 (s, phenyl carbons), 115.5 (s, uncoordinated C₁), 28.9 (overlapping doublet and singlet, J_{P-C} = 19 Hz) and 26.6 ppm (d, J_{P-C} = 20 Hz) (methylene carbons). At -83 °C: 141.8 (s, uncoordinated C₂'), 138.3 (s, uncoordinated C₂), 133.6, 132.2, 131.0, 130.3, 129.5, 128.6 (br s, phenyl carbons), 118.8 (s, uncoordinated C₁'), 115.2 (s, uncoordinated C₁), 75.9 and 39.2 (br s, carborane carbons), 73.3 and 51.5 (s, coordinated C₂' and C₁', respectively), 32.5, 30.9, 29.1, 27.6, 25.1, and 21.3 ppm (br s, methylene carbons). ³¹P{¹H} FT NMR (81.02 MHz, 20% CD₂Cl₂/CH₂Cl₂, 47 °C): 42.8 ppm (br s, W_{1/2} ≈ 160 Hz). At -3 °C: 46.4 ppm (br s, W_{1/2} ≈ 1200 Hz). At -88 °C: 61.0 (d, J_{P-P} = 37 Hz) and 36.5 ppm (d). ¹¹B{¹H} FT NMR (111.8 MHz, CD₂Cl₂, 44 °C): 2.6 (3) and -15.8 ppm (4). At -71 °C: 24.9 (2), -3.4 (2), and -19.9 ppm (3). Infrared spectrum (KBr): ν_{C=C} (uncoordinated) at 1633 cm⁻¹.

Preparation of [closo-6-CO-6,6-(DBP)₂-6,2,3-RuC₂B₇H₉] (Vb). Dry carbon monoxide was bubbled through a solution of [Ru(DBP)₂(C₂B₇H₉)] (IIIf, 0.150 g, 0.232 mmol) in toluene (5 mL), yielding a bright yellow solution. Upon addition of petroleum ether (10 mL) and cooling to -15 °C for 1 day, yellow crystals of [closo-6-CO-6,6-(DBP)₂-6,2,3-RuC₂B₇H₉] (Vb, 0.133 g, 87%) were obtained, mp 121–123 °C. Anal. Calcd for C₃₃H₃₅B₇P₂ORu: C, 55.21; H, 7.02; P, 9.18. Found: C, 54.78; H, 7.14; P, 9.66. ¹H FT NMR (200.133 MHz, C₆D₆): τ 2.40 (m, 2 H), 2.60 and 2.98 (m, 4 H) (phenyl protons), 4.52 (m, 4 H, H₃), 5.11 (d, J₁₃ = 11 Hz, 4 H, H₁), 5.17 (d, J₂₃ = 24 Hz, 4 H, H₂), 6.59 (br s, 2 H, carborane C-H), 8.11 and 8.60 (m, 8 H, methylene protons). ³¹P{¹H} FT NMR (81.02 MHz, 20% CD₂Cl₂-CH₂Cl₂): 29.7 ppm (s). ¹¹B{¹H} FT NMR (80.5 MHz, CD₂Cl₂): 0.00 (2), -9.13 (1), and -23.4 ppm (4). Infrared spectrum (KBr): ν_{CO} at 1930 (s, br) and ν_{C=C} (uncoordinated) at 1632 cm⁻¹ (s).

The complex [closo-6-CO-6,6-(MBP)₂-6,2,3-RuC₂B₇H₉] (Va, 70 mg, 77%) was similarly prepared from [Ru(MBP)₂(C₂B₇H₉)] (93 mg, 0.13 mmol) at -78 °C, mp 174–176 °C (melts to a red liquid, darkens at 165 °C). Anal. Calcd for C₃₅H₄₃B₇P₂ORu: C, 58.52; H, 6.03; P, 8.62. Found: C, 58.18; H, 6.15; P, 8.33. ¹H FT NMR (200.133 MHz, C₆D₆): τ 2.42 (m, 4 H), 2.89 and 3.08 (m, 8 H) (phenyl protons), 4.63 (m, 2 H, H₃), 5.18 (d, J₁₃ = 10 Hz, 2 H, H₁), 5.25 (d, J₂₃ = 17 Hz, 2 H, H₂), 6.70 (br s, 2 H, carborane C-H), 7.79 and 8.04 (m, 4 H, methylene protons). ³¹P{¹H} FT NMR (81.02 MHz, 20% C₆D₆/C₆H₆): 42.5 (s). ¹¹B{¹H} FT NMR (80 MHz, CD₂Cl₂): 0.4 (2), -8.2 (1), and -22.0 ppm (4). Infrared spectrum (KBr): ν_{CO} at 1932 (s, br) and ν_{C=C} (uncoordinated) at 1628 cm⁻¹ (w). The carbonylation of IVa was monitored by ³¹P{¹H} FT NMR at several temperatures, using rubber septa and a syringe needle ([IVa] ≈ 0.03 M). At -78 °C in 10% C₆D₆-C₆H₅CH₃: 45.0 ppm (s). At 30 °C in 10% C₆D₆-C₆H₅: 45.4 (s, 1), 42.5 (s, 5), and -15.3 ppm (s, 1) (≈30% IIIb). At 60 °C in 10% C₆D₆-C₆H₅CH₃ (the sample was carbonylated at 60 °C and the spectrum recorded at 30 °C): 45.5 (s, 1), 42.5 (s, 2), and -15.3 ppm (s, 1) (≈50% IIIb). Infrared

spectrum of IIIb (Nujol): ν_{CO} at 1970 and 2025 cm^{-1} .

Acknowledgments. We wish to thank the National Science Foundation (Grant CHE78-05679) and the Office of Naval Research for their generous support of this work. The authors thank Dr. C. A. O'Con, Dr. D. C. Busby, and Mr. T. B. Marder for assistance in obtaining the ^{11}B , ^1H , and ^{31}P FT NMR spectra, Mr. R. E. King for measurement of the crystal density, Dr. Bradley Katz for assistance with the diffractometer, and Miss Susan Heytens for the illustrations. The Syntex P1 automated diffractometer and the Bruker WP-200 FT NMR spectrometer were

purchased with funds from NSF Grants GP2824 and CHE76-05926, respectively, and computer time was furnished by the UCLA Campus Computing Network.

Supplementary Material Available: Root-mean-square amplitudes of vibration and equivalent B values (Table IV), structure factor amplitudes (Table V), interatomic distances (Table VI), average bond lengths (Table VII), interatomic angles (Table VIII), and selected least-squares planes and interplanar angles (Table IX) (22 pages). Ordering information is given on any current masthead page.

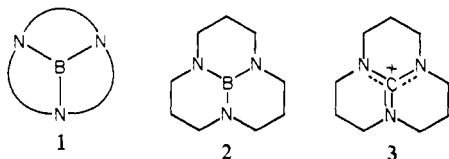
Tris(amino)boranes: The Effect of Angle Strain on Hybridization

Jack E. Richman,* N.-C. Yang, and Leah L. Andersen

Contribution from the Department of Chemistry, University of Idaho, Moscow, Idaho 83843.
Received January 28, 1980

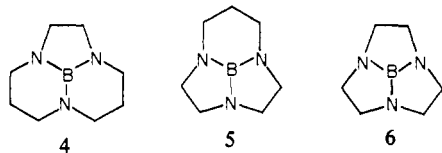
Abstract: The four tris(amino)boranes represented by structure 1 with ethylene and/or trimethylene bridges have been prepared. Predictions that the smallest member of this series, 10-bora-1,4,7-triazatricyclo[5.2.1.0^{4,10}]decane, would be highly strained were supported by the observation that this compound exists only as a tight dimer. 11-Bora-1,4,7-triazatricyclo[5.3.1.0^{4,11}]undecane is dimeric in solution but monomeric in the gas phase. The X-ray crystal structure and properties of 13-bora-1,5,9-triazatricyclo[7.3.1.0^{5,13}]tridecane show that it has a stable planar BN_3 array.

We report experiments pertaining to the effect of angle strain on the hybridization and reactivity of boron-nitrogen bonds. Our results also apply to isoelectronic carbon-nitrogen systems.¹ We have prepared the series of compounds depicted by structure 1 where the curved lines represent ethylene or trimethylene bridges.



The largest member of this series, 2, is isoelectronic with guanidinium ion 3. Models indicate that both 2 and 3 are reasonably unstrained when the four atoms of the central array are trigonal coplanar. Since salts of 3 had previously been prepared^{2,3} and exhibit normal stability, we expected that 2 would represent an especially stable tris(amino)borane.

Structures 4-6 represent three lower homologues of 2 which show increasing strain. Models⁴ suggest that 4, with one less methylene group, is considerably more strained than 2 if the four



(1) For a discussion of the analogy between boranes and carbonium ions, see: Davis, R. E.; Ohno, A. *Tetrahedron* 1967, 23, 1015-28. Davis, R. E.; Murthy, A. S. N. *Ibid.* 1968, 24, 4595-4603.

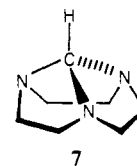
(2) Richman, J. E., presented at the Gordon Heterocycles Conference, New Hampton, NH, June 1974.

(3) Atkins, T. J. "Abstracts of Papers", ACS/CJS Chemical Congress, Honolulu, HI, April 1979; American Chemical Society: Washington, D.C.; ORGN 106.

(4) Dreiding and Framework Molecular Models were used.

atoms of the BN_3 array remain trigonal and coplanar—a geometry that is impossible for 5 and 6, assuming normal bond distances. However, if the three nitrogens of 5 and 6 adopt a pyramidal geometry (sp^3 hybridization), then the BN_3 nuclei can maintain a semblance of coplanarity.

Models also show that a conformation for 6 free of angle strain can be achieved if all four atoms of the BN_3 array adopt a pyramidal geometry—a conformation quite similar to that expected for 7, recently reported³ to be a stable compound. However, this



conformation for 6 requires a *trivalent pyramidal* boron atom, an electronic strain that must be very considerable.^{1,5} The tendency for trivalent boron to remain planar is similar to the tendency for planarity in isoelectronic carbocations.⁵

We report the synthesis of compounds 2, 4, and 5 and properties for these compounds that are consistent with the above considerations. Attempts to synthesize 6 have given only a dimer of this structure.

Results and Discussion

Syntheses. The synthesis of the polycyclic aminoboranes, 1, in each case started with the triaza-monocyclic ring. However, the four compounds described in this paper were best synthesized by three different methods. Compound 2 was prepared in good yield by refluxing 1,5,9-triazacyclododecane⁶ with excess methyl

(5) Jemmis, E. D.; Buss, V.; Schleyer, P. v. R.; Allen, L. C. *J. Am. Chem. Soc.* 1976, 98, 6483-9.

(6) (a) Richman, J. E.; Atkins, T. J. *J. Am. Chem. Soc.* 1974, 96, 2268-70; (b) Koyama, H.; Yoshino, T. *Bull. Chem. Soc. Jpn.* 1972, 45, 481-4.